Reactivity and Efficiency of Difunctional Radical Photoinitiators

C. Dietlin,[1] J. Lalevee,[1] X. Allonas,[1] J. P. Fouassier,[1] M. Visconti,[2] G. Li Bassi,[2] G. Norcini[2]

[1]*Department of Photochemistry, Unité Mixte de Recherche (UMR) 7525 Centre National de la Recherche Scientifique, University of Haute Alsace, Ecole Nationale Supérieure de Chimie de Mulhouse (ENSCMu), 3 Rue Alfred Werner, 68093 Mulhouse Cedex, France*
[2]*Lamberti SpA, Chemical Specialties, Via Piave 18, 21041 Albizzate, Italy*

Received 7 March 2007; accepted 1 June 2007
DOI 10.1002/app.27008
Published online 13 September 2007 in Wiley InterScience (www.interscience.wiley.com).

ABSTRACT: Three difunctional cleavable photoinitiators based on the α-hydroxyketone structure were tested in photopolymerization reactions with Fourier transform infrared spectroscopy. The excited-state processes were investigated with time-resolved laser absorption spectroscopy and laser-induced photocalorimetry, which allowed the cleavage quantum yields to be determined and estimates of the triplet-state lifetimes and interaction rate constants with a methacrylate monomer to be given. Modeling calculations helped to describe the ground-state properties and showed that the difunctional photoinitiators exhibited different chromophoric groups than the corresponding monofunctional photoinitiator. An examination of the photochemical reactivity versus the practical efficiency observed in the polymerization showed that these difunctional photoinitiators exhibited better efficiency than the parent molecule, mainly because of their increased absorption properties. Their practical efficiency appeared to be better because of better light absorption when standard polychromatic light sources were used. © 2007 Wiley Periodicals, Inc. J Appl Polym Sci 107: 246–252, 2008

Key words: photochemistry; photophysics; photopolymerization

INTRODUCTION

The design of suitable photoinitiators (PIs) has received considerable attention in the last 2 decades. Many aspects have been explored, such as the effects of the skeletons and substituents in inducing improved properties.[1] In specific areas, such as graphic arts and conventional clear-coat and overprint varnish applications, PIs must exhibit particular properties: a high photochemical reactivity leading to high curing speeds even in pigmented formulations (usable as inks) and the formation of low-volatility photolysis products that should present no yellowing, no migration, and no residual odor. Difunctional photoinitiators (DiPI),[2–6] multifunctional PIs,[7] polymeric PIs,[8,9] and bifunctional PIs[10] have been proposed so far for useful applications, whereas only a few studies of the performance attained as a function of the chemical structure have been proposed.[11–16] In a recent article,[17] the state of the art was reviewed; among the various proposed systems, a few have led to useful applications, such as bis(2,4,6-trimethylbenzoyl)phenyl-phosphine oxide, oligo-(2-hydroxy-2-methyl-1-[4-(1-methylvinyl)phenyl]-propan-1-one, oxophenylacetic acid 2-[2 oxo-2-phenylacetoxyethoxy]ethyl ester, bis-1,14-(thioxanthone-2-oxyacetyl)-tributylene-glycol, bis-1,14-(benzophenone-4-oxyacetyl)-tributylene-glycol, and 1-[4-(4-benzoylphenylsulfonyl]-2-methyl-2-(4-methylphenylsulfonyl)-propan-1-one.

Very recently, radical DiPIs based on the α-hydroxyketone structure have been developed for clear-coating applications;[3,4] they are claimed to exhibit very high practical efficiency, low postcuring odor, and low migration of the photolysis products. One interesting question is to whether this practical efficiency can be ascribed to better photochemical reactivity of DiPIs in comparison with monofunctional PIs. In this article, we use time-resolved laser spectroscopy and molecular modeling to investigate the excited-state processes of three selected derivatives. The photochemical reactivity and polymerization initiation ability of these derivatives in comparison with the monofunctional parent compound are discussed in detail.

EXPERIMENTAL

The formulas of the studied compounds are displayed in Chart 1. 2-Hydroxy-2,2-dimethylacetophenone (HK; Irgacure 1173, Ciba Specialty (Basel, Switzerland), or Esacure KL200, Lamberti, Gallarte, Italy) was used as a reference compound. 2-Hydroxy-1-[4-4-(2-hydroxy-2-methylpropionyl)phenoxy)phenyl]-2-methyl-1-one (HK-o),[18] bis[4-(2-hydroxy-2-methylpropionyl)phenyl]methane (HK-c; Irgacure 127, Ciba C1

Correspondence to: X. Allonas (xavier.allonas@uha.fr).

Journal of Applied Polymer Science, Vol. 107, 246–252 (2008)

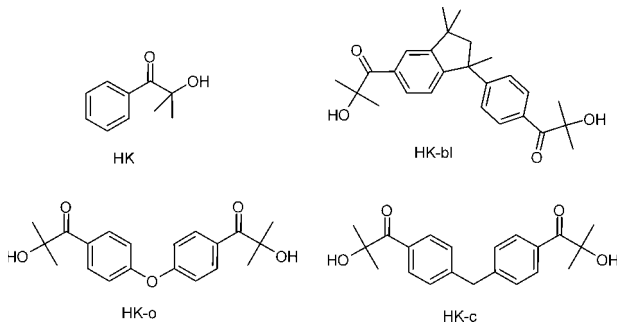

Chart 1. Formulas and abbreviations of the studied compounds. For HK-bl, the hydroxy isopropyl group is not defined (the 5- or 6-position).

Specialty),[4] and a mixture of 2-hydroxy-1-[4-(5-(2-hydroxy-2-methylpropionyl)-1,3,3-trimethylindan-1yl) phenyl]-2-methyl propan-1-one and 2-hydroxy-1-[4-(6-(2-hydroxy-2-methylpropionyl)-1,3,3-trimethylindan-1yl)phenyl]-2-methyl-propan-1-one (HK-bl; Lamberti)[19] were gifts from Lamberti and used as received.

The laser flash photolysis system used for the excited-state experiments was based on a nanosecond optical parametric oscillator (Sunlite, Continuum, Santa Clara, CA) pumped by an Nd : Yag laser (Powerlite 9010, Continuum). The analyzing system used a 450-W pulsed xenon arc lamp, a Czerny-Turner monochromator, and a fast photomultiplier (LP900, Edinburgh Instruments, Livingston, UK).[16] The experimental setup of the laser induced photoacoustic calorimetry (LIPAC) has been fully described elsewhere:[20] the attenuated beam of a frequency-tripled nanosecond Nd : YAG laser (Powerlite 9010, Continuum) irradiated a 1-cm cell equipped with a Panametrics (Billerica, MA) piezoelectric detector (A609S, 5 MHz, or A603S, 1 MHz) through a 200- or 500-μm pinhole; the amplified signal was monitored by a transient digitizer (3052, Tektronix, Tokyo, Japan).

The molecular orbital calculation procedures were carried out with the Gaussian suite of programs[21] according to a procedure described elsewhere.[22] Density functional theory was used to calculate the structure of the molecule. The relaxed ground state and radicals produced after cleavage were fully optimized with the B3LYP functional with the 6-31G* basis set. The absorption properties were computed with a time-dependent method at a PBE1PBE/6-311++G** level and a B3LYP/6-311++G** level.

The polymerizable formulation was based on a 75/25 (w/w) mixture of bisphenol A epoxy acrylate and tripropylene glydol diacrylate (Ebecryl 605, Cytec, West Paterson, NJ). All the experiments were carried out with a formulation sandwiched between two polypropylene films (~ 100 μm thick). The polymerization reactions were conducted under exposure to a xenon–mercury lamp (LC5, Hamamatsu, Shizuoka Pref., Japan) with either a polychromatic light

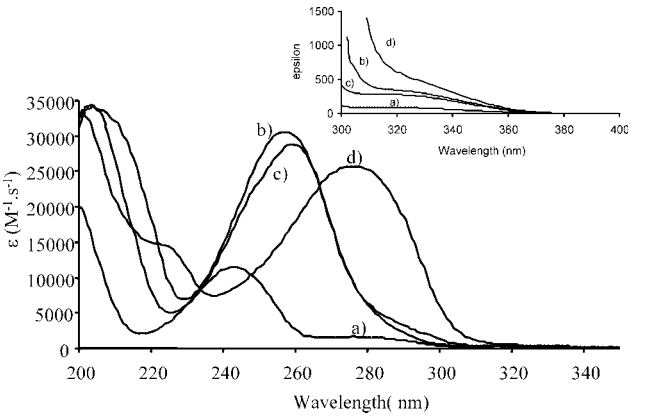

Figure 1 Typical ground-state absorption spectra of the compounds in acetonitrile: (a) HK, (b) HK-bl, (c) HK-c, and (d) HK-o.

(intensity ≈ 0.7 mW/cm^2) or a 366-nm monochromatic light (intensity ≈ 0.2 mW/cm^2). The conversion of the monomer was followed by the monitoring of the disappearance of the IR absorption of the acrylate double bond at 1635 cm^{-1} [16] with real-time Fourier transform infrared spectroscopy (Nexus 870, Nicolet, Waltham, MA).

RESULTS AND DISCUSSION

Ground-state absorption spectra

Typical ground-state absorption spectra are presented in Figure 1, and the molar extinction coefficient (ε) values at the absorption maxima are gathered in Table I. It must be emphasized that the ε values reported in Table I have been calculated with concentrations expressed as moles per liter. If one considers that there are two independent PI units per molecule, the ε values should be in an approximately 2-fold ratio. This is not the case. The observed absorption bands of all the compounds clearly correspond to π–π* and *n*–π* transitions. The *n*–π* transitions appear as a small shoulder above 320 nm. The maxima of the π–π* transitions are red-shifted compared with that of HK. These results suggest that the two chromophoric groups cannot be considered isolated. A partial charge transfer in the electronic transitions can occur in HK-o along the π system of the molecule, as is already known for

TABLE I
Values of the Molar Extinction Coefficient at 366 nm (ε_{366}) and the Wavelength (λ_{max}) and Extinction Coefficient (ε_{max}) at the Absorption Maximum for Experiments Performed in Acetonitrile

	HK	HK-c	HK-bl	HK-o
ε_{366} (mol^{-1} L cm^{-1})	9.6	24.8	29.6	33.5
ε_{max} (mol^{-1} L cm^{-1})	11,515	28,820	30,615	25,750
λ_{max} (nm)	243	260	257	276

TABLE II
Absorption Properties

HK		HK-o		HK-c		HK-bl	
Wavelength (nm)[a]	Wavelength (nm)[b]	Wavelength (nm)[a]	Wavelength (nm)[b]	Wavelength (nm)[a]	Wavelength (nm)[b]	Wavelength (nm)[a]	Wavelength (nm)[b]
338 (0.0003)	343 (0.0003)	336 (0.0018)	341 (0.0024)	337 (0.0003)	343 (0.0003)	331 (0.0007)	335 (0.0007)
		335 (0.0003)	340 (0.0003)	331 (0.0008)	335 (0.0008)	329 (0.0005)	334 (0.0005)
257 (0.0242)	264 (0.0240)	289 (0.6043)	300 (0.5446)	270 (0.2248)	280 (0.2174)	276 (0.1400)	286 (0.1899)
240 (0.1968)	248 (0.1134)	262 (0.3410)	275 (0.0437)	262 (0.1810)	270 (0.1379)	273 (0.1983)	283 (0.0658)

The oscillator strengths are in parentheses.
[a] Computed at the PBE1PBE/6-311++G** level on a B3LYP/6-31G* optimized geometry.
[b] Computed at the B3LYP/6-311++G** level on a B3LYP/6-31G* optimized geometry.

related compounds in which the benzoyl group is substituted by a thioether, amino, or ether group.[1(e)] In HK-c and HK-bl, this is obviously not possible.

The results of the quantum mechanical calculations are gathered in Table II. The first two computed low-energy transitions are localized in the same wavelength region (ca. 340 nm) for all the molecules and exhibit an n–π* character. Concerning the third transition (π–π* transition), the two methods give results differing by about 10 nm. The B3LYP functional correctly fits the absorption properties of HK, but the other molecules are better fitted with the PBE1PBE functional. The n–π* transitions are not strongly modified by the coupling of two HK moieties. On the other hand, the π–π* transitions of the difunctional molecules are redshifted (by 30–40 nm) in comparison with HK. The calculated wavelengths are in good agreement with the experimental ones, the difference being about 15 nm for the DiPIs and 5 nm for HK. These results confirm that DiPIs do not behave like two independent HK molecules: they should be considered to be exhibiting different chromophoric groups. The charge transfer in the difunctional molecules is probably responsible for the increase in the systematic error between experimentation and computation, the time-dependent density functional theory (TDDFT) methods being known to be less accurate in that case.[23]

A study of the molecular orbitals of the four compounds allows a better explanation of these results

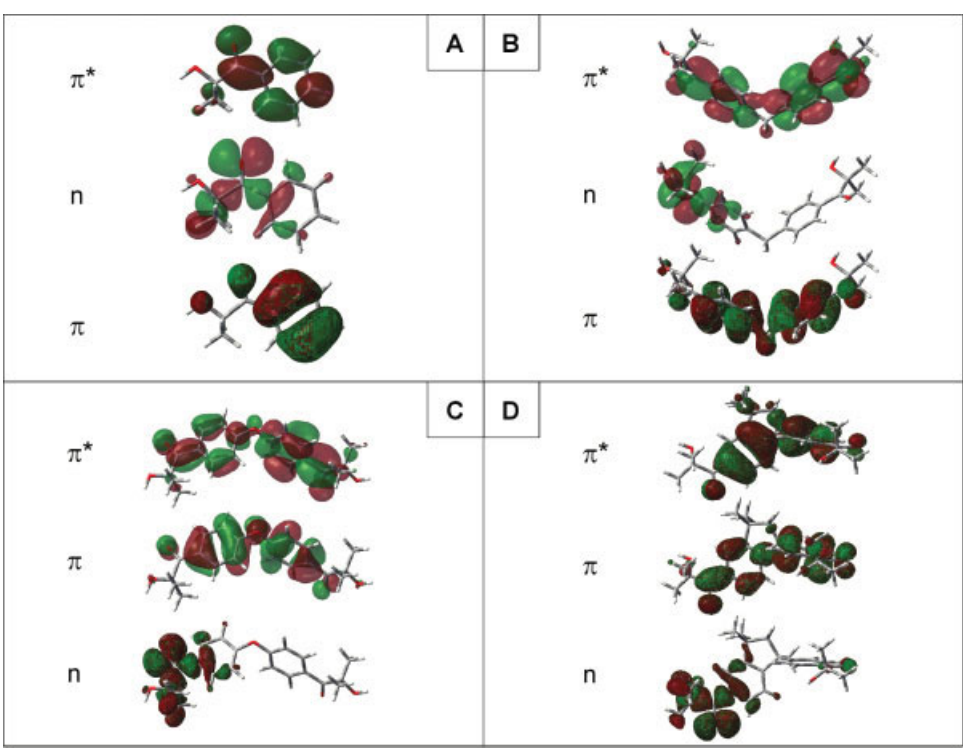

Figure 2 Calculated main n, π, and π* molecular orbitals of (A) HK, (B) HK-c, (C) HK-o, and (D) HK-bl at a BLYP/6-31G* level. For parts C and D, the energy difference between the n and π orbitals is low (<0.3 eV). [Color figure can be viewed in the online issue, which is available at www.interscience.wiley.com.]

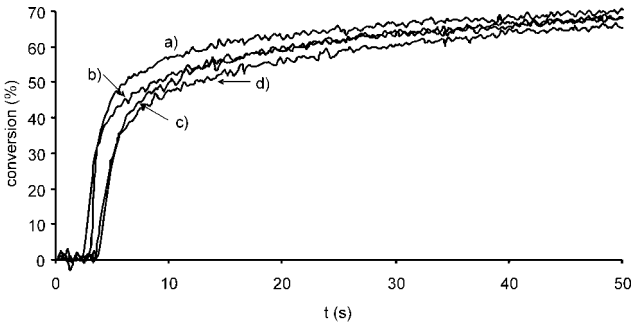

Figure 3 Typical photopolymerization profiles obtained in the presence of 1% (a) HK-o, (b) HK-bl, (c) HK, and (d) HK-c under polychromatic light.

(Fig. 2). The *n* orbitals are localized only on one of the two benzoyl groups of the difunctional molecules, but the π orbitals are delocalized over the entire molecule. This could explain why the π–π* transitions are more affected than the *n*–π* transitions by the coupling of two HK moieties. The delocalization of the π orbitals takes place through a conjugative interaction with the 2π orbital of the oxygen atom in HK-o. This is obviously not possible in HK-bl and HK-c. In that case, a through-space hyperconjugation takes place: the molecule is slightly twisted to allow the coupling of the two π systems.

Therefore, the DiPIs exhibit different absorption properties than the parent molecule because of electronic delocalization and hyperconjugation over the two chromophoric groups.

Polymerization activity of the different derivatives

Examples of photopolymerization profiles are displayed in Figure 3, and relative rates of polymerization are reported in Table III. Under excitation at 366 nm, it is possible to correct the relative rates of polymerization for the different amounts of light absorbed by the molecules. The corresponding corrected values appear to be almost similar for HK and the three DiPIs; this means that one photon absorbed yields the same polymerization activity whatever PI is used. In other words, under excitation at 366 nm, the photochemical reactivity of the DiPI is not affected compared with that of the monofunctional PI.

On the contrary, under polychromatic light excitation, the three DiPIs exhibit better efficiency than the reference compound. HK-o and HK-bl appear to be the best ones, likely because of the higher amount of energy absorbed at a given weight concentration. HK-c and HK basically lead to similar results. These data emphasize how the difunctional derivatives are very attractive from a practical point of view.

Excited-state processes

It is well known that HK undergoes the generation of two radicals through fast cleavage in the triplet state.[1,22] The same behavior should be expected in the corresponding DiPIs. The direct observation of these triplet states and radicals by time-resolved laser spectroscopy is rather difficult,[22] and the processes involved can be studied through indirect methods based on the reactions of Scheme 1.

The triplet-state lifetime (τ) values can be calculated from quenching experiments with naphthalene with eqs. (1) and (2). The increase in the optical density of the naphthalene triplet formation in deaerated benzene at 420 nm was monitored by laser flash photolysis (Fig. 4). The results reported in Table IV show that the calculated τ values (with the energy transfer rate constant of the DiPI with naphthalene, $k_1 = 7.10^9$ mol^{-1} l s^{-1} [24]) are short. The very short values (<1 ns) are not accurate with this procedure; the correct value for HK is 0.45 ns:[22,24]

$$1/\mathrm{OD}_{3\mathrm{N}} = A[1 + k_0/k_1(1/[\mathrm{N}])] \quad (1)$$

$$k_0 = 1/\tau_0 \quad (2)$$

where $\mathrm{OD}_{3\mathrm{N}}$ is the optical density of the naphthalene triplet monitored at 420 nm, A is a constant and k_0 is the cleavage rate constant and [N] is the naphthalene concentration in equation (1).

TABLE III
Relative Rates of Polymerization and Final Conversions Obtained in the Presence of the Various Photoinitiating Systems upon Exposure to a Monochromatic Light or a Polychromatic Light

	Polychromatic light[a]		Monochromatic light[b]	
Formulation	Rate of polymerization (au)	Conversion (%)	Rate of polymerization (au)	Conversion (%)
HK	100	83	100	97
HK-c	100	82	100	96
HK-bl	130	83	110	95
HK-o	180	83	100	95

All values were normalized with 100 used for the reference compound HK.
[a] The formulations contained 1% (w/w) PI in Ebecryl 605.
[b] The formulations contained 5% (w/w) PI in Ebecryl 605. The rates determined under monochromatic light at 366 nm were corrected for the difference in the energy absorbed by the samples.

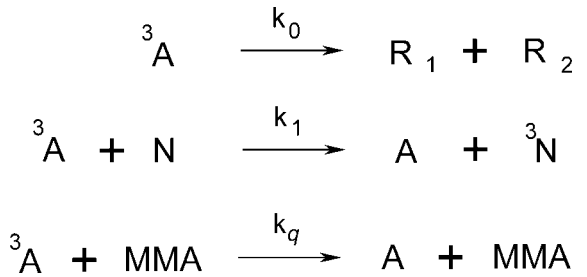

Scheme 1 Energy-transfer reaction.

The decrease in the naphthalene triplet optical density at 420 nm was also monitored (Fig. 5) as a function of the methyl methacrylate (MMA) concentration [optical density of MMA (OD_{MMA})] according to eq. (3) (OD_0 corresponds to [MMA] = mol·l^{-1}). The values of the MMA quenching rate constant (k_q; Table IV) can be obtained by the plotting of OD_0/OD_{MMA} as a function of the MMA concentration:

$$OD_0/OD_{MMA} = 1 + \{k_q/(k_1[N] + k_0)\}[MMA] \quad (3)$$

Photoacoustic calorimetry was employed to measure the cleavage quantum yield (ϕ_c) of the studied molecule in an argon-saturated acetonitrile solution (optical density at 355 nm = 0.17). The amplitude of the acoustic wave (a_1), extrapolated at a zero pump intensity (Fig. 6), is proportional to all the fast heat released by the nonradiative deactivation pathways,[20(b)] including the cleavage reaction [eq. (4)]. Hydroxybenzophenone (BPOH) was used as a reference to calibrate the system (a_{ref}). Molecular modeling was performed to calculate the bond dissociation energy (BDE) at a B3LYP/6-31G* level from the energy of the two radicals produced ($E(R_1)$ and $E(R_2)$) and from the ground state energy of the DiPI ($E(A)$). With the BDE values, ϕ_c can be deduced with eq. (5) (Table IV). For these systems, the error in the BDE is weak in comparison with the use of isodesmic reactions. Interestingly, all the compounds exhibit a ϕ_c value close to unity (Table IV), and this emphasizes that the delocalization or hyperconjugation over the entire molecule of DiPI does not affect the cleavage process:

$$S_{Fast} = E_{h\nu} \times a_1/a_{ref} \quad (4)$$

$$E_{h\nu} - S_{Fast} = \phi_c \times BDE \quad (5)$$

where $E_{h\nu}$ is the energy of the photon absorbed by the molecule and S_{Fast} is the fast heat released by the nonradiative deactivation pathways.

TABLE IV
τ, k_q, BDE, and ϕ_c Values

	τ (ns)[a]	10^{-9} k_q (mol^{-1} L s^{-1})[b]	BDE (kcal/mol)[c]	ϕ_c
HK	0.8[d]	2.1	64.1	0.85
HK-c	1.9	1	63.1	0.9
HK-bl	3	1	69.4	0.8
HK-o	7	0.4	57.1	1

[a] Calculated from quenching experiments with naphthalene in benzene.
[b] In naphthalene/sample benzene solutions.
[c] BDE = $E(R_1) + E(R_2) - E(A)$ (computed at a B3LYP/6-31G* level).
[d] See the text.

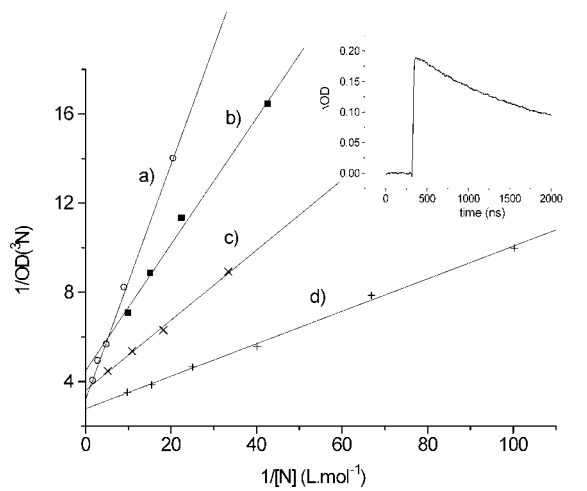

Figure 4 Plot of the reciprocal optical density (1/OD) at 420 nm versus the reciprocal value of the naphthalene concentration ([N]) in (a) HK, (b) HK-c, (c) HK-bl, and (d) HK-o solutions in benzene (optical density = 0.5 at 355 nm) under argon. The inset shows typical naphthalene triplet kinetics. The OD_{3N} values were measured 100 ns after the laser pulse.

DISCUSSION

The initiation of the polymerization occurs through the processes shown in Scheme 2.

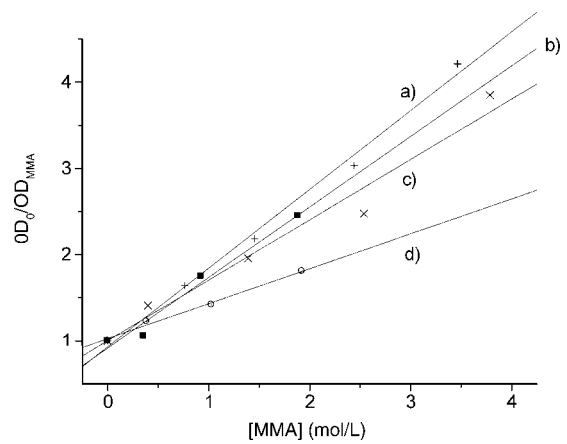

Figure 5 Plot of OD_0/OD_{MMA} at 420 nm versus the MMA concentration in (a) HK-o, (b) HK-c, (c) HK-bl, and (d) HK deaerated benzene solutions in the presence of 0.1–0.5 mol/L naphthalene. The optical densities were measured 100 ns after the laser pulse.

The rate of polymerization (R_p) is a function of the initiation quantum yield (ϕ_i):

$$R_p = K\sqrt{\phi_i} \tag{6}$$

ϕ_c can be expressed as follows:

$$\phi_c = \phi_{\mathrm{ISC}} \frac{k_c}{k_c + k_q[\mathrm{M}]} \tag{7}$$

where Φ_{ISC} is the quantum yield of intersystem crossing, [M] is the monomer concentration and k_q is the quenching rate constant, and k_c is the cleavage rate constant, which is very often assumed to be equal to the reciprocal value of τ. ϕ_i is defined as $\phi_i = \phi_c \times \phi_{RM}$, where ϕ_{RM} represents the yield of the first monomer radicals. The increase in the viscosity in bulk lowers the monomer quenching, which consequently should not compete with the cleavage process. Because of the high ϕ_c values, one can reasonably conclude that the productions of initiating radicals in the DiPIs and HK are not significantly different. The efficiency of the addition of the isopropyl ketyl radical (which is the main initiating species) to an acrylate unit will obviously be unaffected by the kind of derivative. The reactivity of the substituted benzoyl radical might be changed to some extent. The contribution of these radicals should be diffusion-limited ($\sim 10^5$ M^{-1} s^{-1} in Ebecryl 605[25]). Therefore, no strong modification of the photochemical reactivity of these DiPIs in comparison with HK has been observed, in agreement with the conclusion drawn from photopolymerization experiments carried out under monochromatic light exposure. On the contrary, the change in the ground absorption spectra as well as the values of ε leads to a higher amount of absorbed energy, and this explains the higher rates of polymerization obtained upon exposure to polychromatic lights.

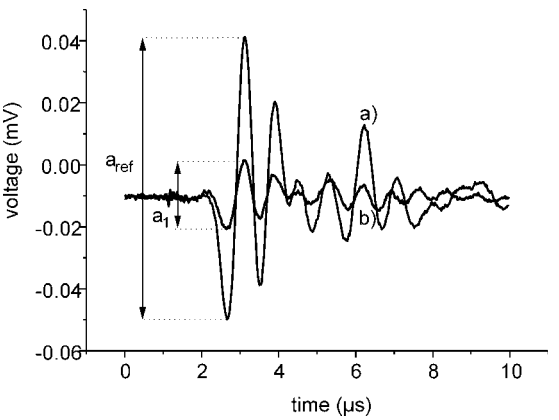

Figure 6 Photoacoustic waves of (a) BPOH and (b) HK-o in acetonitrile. The optical density was 0.17 at 355 nm. a_{ref} and a_1 are the BPOH and HK-o amplitudes of the photoacoustic waves, respectively.

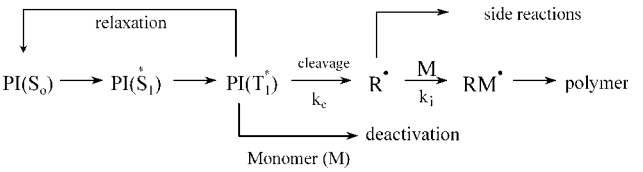

Scheme 2 Initiation reaction.

CONCLUSIONS

This article shows that DiPIs do not behave as two isolated functional units containing a PI. As revealed by molecular modeling, a delocalized chromophoric group is present in such a DiPI structure that allows better light absorption without any noticeable detrimental effect on the excited-state processes. As a result, the rates of polymerization obtained with DiPIs are higher than those with monofunctional PIs. In addition, these compounds, as they exhibit lower migration in cured coatings, are very attractive from an industrial point of view.

References

1. (a) Fouassier, J. P. Photoinitiation, Photopolymerization, Photocuring; Hanser: Munich, 1995; (b) Radiation Curing and Polymer Science and Technology; Fouassier, J. P.; Rabek, J. F., Eds.; Chapman & Hall: Andover, MN, 1993; (c) Davidson, S. Exploring the Science, Technology and Application of UV and EB Curing; Sita Technology: London, 1999; (d) Photoinitiated Polymerization; Belfied, K. D.; Crivello, J. V., Eds.; ACS Symposium Series 847; American Chemical Society: Washington, DC, 2003; (e) Dietliker, K. A Compilation of Photoinitiators Commercially Available for UV Today; Sita Technology: London, 2002; (f) Photochemistry and UV Curing; Fouassier, J. P., Ed.; Research Signpost: Trivandrum, India, 2006.
2. Visconti, M.; Belloti, E.; Cattaneo, M. Proc RadTech Eur 2005, 2, 313.
3. Visconti, M.; Cattaneo, M. Proc RadTech Eur 2003, 1, 205.
4. Fuchs, A.; Husler, R.; Schregenberger, C.; Kunz, M. (to Ciba Specialty). PCT Int. Appl. WO 03/040076 (2003).
5. Fuchs, A.; Bolle, T.; Ilg, S.; Husler, R. Proc RadTech Eur 2003, 1, 507.
6. Herlihy, S. L.; Schaun, L. PCT Int. Appl. WO 03 72,568 (2003).
7. Herlily, S. Proc RadTech USA 2002, 1, 413.
8. Visconti, M.; Norcini, G.; Li Bassi, G. PCT Int. Appl. WO 02 85,832 (2002).
9. Bertens, F. Proc RadTech Eur 2005, 1, 473.
10. Visconti, M. Proc RadTech 2002, 1, 1033.
11. Corrales, T.; Catalina, F.; Peinado, C.; Allen, N. S. J Photochem Photobiol A 2003, 159, 103.
12. Angiolini, L.; Caretti, D.; Carlini, C.; Corelli, E.; Salatelli, E. Polymer 1999, 40, 7197.
13. Liska, R. J Polym Sci Part A: Polym Chem 2002, 40, 1504.
14. Pouliquen, L.; Coqueret, X.; Morlet Savary, F.; Fouassier, J. P. Macromolecules 1995, 28, 8028.
15. Fouassier, J. P.; Lougnot, D. J.; Li Bassi, G.; Nicora, C. Polymer Commun 1989, 30, 245.
16. Fouassier, J. P.; Allonas, X.; Lalevée, J.; Visconti, M. J Polym Sci Part A: Polym Chem 2000, 38, 4531.

17. Visconti, M. In Photochemistry and UV Curing; Fouassier, J. P., Ed.; Research Signpost: Trivandrum, India, 2006.
18. Norcini, G.; Romagnano, S.; Visconti, M.; Li Bassi, G. (to Lamberti). PCT Int. Appl. WO 05/040083 (2005).
19. Visconti, M.; Norcini, G.; Li Bassi, G. (to Lamberti). PCT Int. Appl. WO 02/085832 (2002).
20. (a) Allonas, X.; Lalevée, J.; Fouassier, J. P. In Photoinitiated Polymerization; Belfield, K. D.; Crivello, J. V., Eds.; ACS Symposium Series 847; American Chemical Society: Washington, DC, 2003; Chapter 12; (b) Allonas, X.; Lalevée, J.; Fouassier, J. P. J Photochem Photobiol A 2003, 159, 127; (c) Lalevee, J; Allonas, X.; Fouassier, J. P. J Am Chem Soc 2002, 124, 9613.
21. (a) Frisch, M. J.; Trucks, G. W.; Schlegel, H. B.; Scuseria, G. E.; Robb, M. A.; Cheeseman, J. R.; Zakrzewski, V. G.; Montgomery, J. A., Jr.; Stratmann, R. E.; Burant, J. C.; Dapprich, S.; Millam, J. M.; Daniels, A. D.; Kudin, K. N.; Strain, M. C.; Farkas, O.; Tomasi, J.; Barone, V.; Cossi, M.; Cammi, R.; Mennucci, B.; Pomelli, C.; Adamo, C.; Clifford, S.; Ochterski, J.; Petersson, G. A.; Ayala, P. Y.; Cui, Q.; Morokuma, K.; Salvador, P.; Dannenberg, J. J.; Malick, D. K.; Rabuck, A. D.; Raghavachari, K.; Foresman, J. B.; Cioslowski, J.; Ortiz, J. V.; Baboul, A. G.; Stefanov, B. B.; Liu, G.; Liashenko, A.; Piskorz, P.; Komaromi, I.; Gomperts, R.; Martin, R. L.; Fox, D. J.; Keith, T.; Al-Laham, M. A.; Peng, C. Y.; Nanayakkara, A.; Challacombe, M.; Gill, P. M. W.; Johnson, B.; Chen, W.; Wong, M. W.; Andres, J. L.; Gonzalez, C.; Head-Gordon, M.; Replogle, E. S.; Pople, J. A. Gaussian 98, Revision A.11; Gaussian: Pittsburgh PA, 2001; (b) Foresman, J. B.; Frisch, A. Exploring Chemistry with Electronic Structure Methods, 2nd ed.; Gaussian: Pittsburgh PA, 1996.
22. Allonas, X.; Morlet Savary, F.; Lalevée, J.; Fouassier, J. P. Photochem Photobiol 2006, 82–88
23. (a) Browman, M.; Pople, S. Computing Studies in Context; Heinemann Educational Secondary Division, Auckland, New Zealand; 1988; (b) Cai, Z. L.; Crossley, M.; Reimers, J.; Kobayashi, R.; Amos, R. J Phys Chem B 2006, 110, 15624.
24. Jockusch, S.; Landis, M. S.; Freiermuth, B.; Turro, N. J. Macromolecules 2001, 34, 1619.
25. Lalevée, J.; Allonas, X.; Jradi, S.; Fouassier, J. P. Macromolecules 2006, 39, 1872.